## PAPER

# Design of peptide therapeutics as protein–protein interaction inhibitors to treat neurodegenerative diseases†

Daryl Ariawan, [iD] ‡ Kanishka P. M. Thananthirige, [iD] ‡ Ali El-Omar, Julia van der Hoven, Sian Genoud, Holly Stefen, Thomas Fath, [iD] Janet van Eersel, [iD] Lars M. Ittner and Ole Tietz [iD] *

Peptide therapeutics are an emerging class of drugs to treat neurodegenerative diseases by inhibiting protein–protein interactions (PPIs). Nerinetide has recently emerged as a promising therapeutic for the treatment of ischemic stroke and Alzheimer's Disease (AD). The design of this potent neuroprotective agent includes a cell penetrating peptide sequence that achieves delivery into neurons and a protein–protein inhibitory sequence that achieves inhibition of protein complex formation through mimicry. In this study, we deconstruct the nerinetide sequence and study the relationship between plasma stability, intraneuronal delivery and drug efficacy to provide design guidelines for the development of next generation, peptidic PPI inhibitors to treat neurodegenerative diseases.

## Introduction

Peptides are a promising class of therapeutics with more than 80 drugs currently used to treat diseases including diabetes, cancer, osteoporosis, multiple sclerosis, and chronic pain.[1] The important role of several endogenous peptides such as neurotensin, oxytocin, and neuropeptide Y in the central nervous system (CNS) has fuelled drug discovery research into the use of peptides to treat CNS indications.[2] Two major hurdles in peptide drug discovery are the short *in vivo* half life of most peptides and their inability to penetrate biological barriers such as the plasma membrane. These issues are particularly pertinent in the development of therapeutic peptides for CNS diseases because agents must penetrate the blood–brain barrier (BBB) to access CNS targets, which in turn requires longer circulation times to allow adequate bioavailability.[3,4]

Nerinetide, also known as Tat-NR2B9c or NA-1, is a synthetic eicosapeptide that has been shown to offer strong protection against excitotoxic damage caused by ischemic stroke in rats as well as non-human primates.[5–7] Furthermore, we showed that nerinetide prevents excitotoxicity-induced cognitive deficits and prolongs survival of a genetic mouse model of Alzheimer's disease (AD).[8] The design of nerinetide is inspired by the discovery that *N*-methyl-ᴅ-aspartate (NMDA) receptors in the

CNS interact with postsynaptic density protein 95 (PSD-95) through an intraneuronal C-terminal domain containing a terminal SXV motif which affects the plasticity of excitatory synapses.[9] Nerinetide disrupts this interaction by mimicking the SXV motif of the NR2B subunit of NMDAR and therefore functions as a protein–protein interaction (PPI) inhibitor by binding to PSD-95 and blocking its interaction with NR2B. Delivery into the CNS and into neurons was achieved through inclusion of the cell penetrating peptide Tat (YGRKKRRQRRR). The 11 amino acids of Tat are conjugated to 9 amino acids of the terminal SXV motif of NMDAR subunit NR2B (KLSSIESDV) to constitute nerinetide (Tat-NR2B9c).

The efficacy and safety of nerinetide were evaluated in a placebo controlled, multicentre clinical trial of acute ischaemic stroke (ESCAPE-NA1) which reported a good safety profile but no improvement in clinical outcomes.[10] These findings were partially attributed to rapid degradation of the peptide in human plasma, particularly upon co-treatment with Alteplase® (=recombinant tissue plasminogen activator (tPA)), which is standard of care treatment for acute ischemic stroke.[11] Further clinical trials, ESCAPE-NEXT and FRONTIER, have recently concluded, promising further insight into efficacy profiles and encouraging the development of novel neuroprotective peptides.[12,13]

Despite the initial clinical trial finding, nerinetide is a potent neuroprotective drug that successfully addresses two significant challenges in the design of peptides as CNS therapeutics: (i) delivery – the inclusion of cell penetrating peptide Tat achieves delivery into the CNS and into neurons; (ii) protein–protein inhibition – a mimetic peptide sequence of one of the interacting proteins achieves inhibition of protein complex

*Dementia Research Centre, Macquarie Medical School, Faculty of Medicine, Health and Human Sciences, Macquarie University, North Ryde, Sydney, NSW 2109, Australia. E-mail: ole.tietz@mq.edu.au*

‡ These authors contributed equally.

formation. While the plasma stability of nerinetide remains a challenge[11] and its use for other CNS indications an open question,[8] the combination of cell penetrating peptide and short protein mimetic sequence is a powerful blueprint for the design of intraneuronal PPI inhibitory therapeutics.

Here we provide insight into the design of next generation neuroprotective peptides by deconstructing the nerinetide sequence and studying the relationship between plasma stability, intraneuronal delivery and drug efficacy.

## Results

### Synthesis of nerinetide peptides

To delineate the contribution of nerinetide functional portions to neuronal uptake and efficacy, we divided the peptide into a C-terminal cell penetrating peptide (CPP) section and an N-terminal PPI inhibitor (PPIi) part (Fig. 1A). The CPP section consists of the archetypical cell penetrating peptide Tat

(YGRKKRRQRRR), while the PPIi section consists of the NMDA receptor NR2B9c motive (KLSSIESDV),[5] resulting in dissection between R11 and K12. To enable detection and tracking of nerinetide sections, peptides were N-terminally labelled with TAMRA ($\lambda_{ex}$ 552 nm; $\lambda_{em}$ 578 nm), giving rise to CPP section peptide TAMRA-Tat and PPI section peptide TAMRA-NR2B9c (Fig. 1B; peptides **1** & **2**). Further, we synthesized TAMRA-D-Tat, a CPP variant of Tat that consists of D-amino acids and more resistant to degradation by proteases than L-amino acid Tat, and TAMRA-NR2Baa, a double alanine mutant version of NR2B9c that is known not to bind to PSD95 (Fig. 1B; peptides **3** & **4**). Finally, we synthesized three TAMRA labelled full length versions of nerinetide – unmodified nerinetide (TAMRA-Tat-NR2B9c), double alanine mutant nerinetide (TAMRA-Tat-NR2Baa), and a D-amino acid/L-amino acid hybrid nerinetide (TAMRA-D-Tat-NR2B9c) where the Tat sequence is composed of D-amino acids and the NR2B9c sequence is composed of L-amino acids (Fig. 1B; peptides **6, 7, 8**).

### Peptide plasma stability

We investigated the stability of Tat-NR2B9c (nerinetide) and D-Tat-NR2B9c in mouse plasma and quantified the percentage of intact peptide at time points 15 min, 30 min, 60 min, 120 min and 300 min using analytical high performance liquid chromatography (HPLC). We observed rapid degradation of Tat-NR2B9c in this assay which is likely due to protease cleavage of the Tat portion of the peptide, as previously demonstrated.[11] The half-life of Tat-NR2B9c in mouse plasma is ~60 min, which drops to <10 min when Alteplase® is added (Fig. 2). Substitution of L-Tat with D-Tat improves the stability of nerinetide significantly; D-Tat-NR2B9c is 90% intact after 300 min and addition of alteplase did not affect degradation (Fig. 2). D substitution of the Tat sequence on nerinetide is a viable strategy to enhance peptide stability.

### Uptake of peptides into live neurons

Stability data in hand, we went on to investigate whether the substitution of D-Tat for L-Tat affects uptake of peptides into neurons. Neuronal uptake and intracellular distribution of peptides (outlined in Fig. 1) were investigated by performing live-cell confocal microscopy of mature murine primary neurons incubated with TAMRA labelled peptide (1, 5 & 10 µM) in neurobasal medium (60 min). Following washing, images
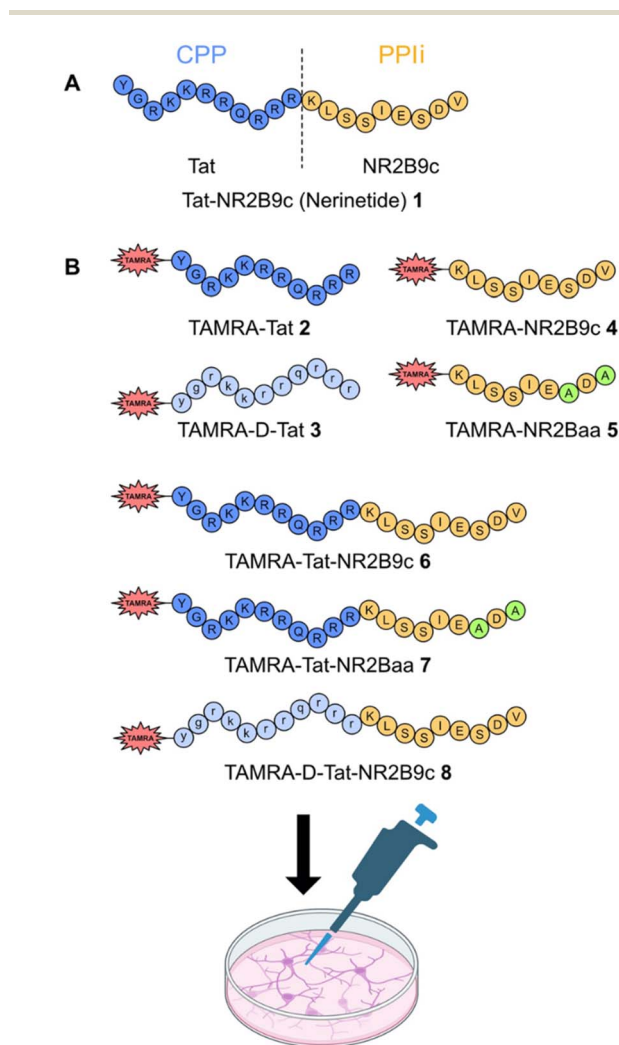


Fig. 1 Overview of peptides used in this study. (A) Structure of nerinetide (**1**) and (B) TAMRA labelled analogues of nerinetide (**6**), nerinetide fragments (**2, 4**) D-Tat (**3**), D-Tat-NR2B9c (**8**), and inactive nerinetide PPIi (**5, 7**).
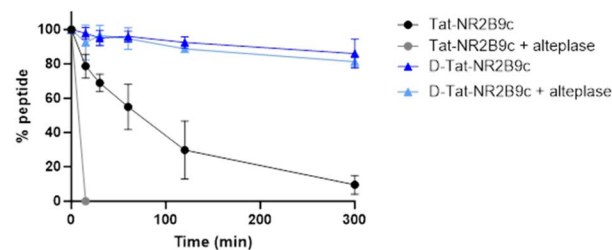


Fig. 2 Mouse plasma stability of nerinetide (Tat-NR2B9c) and D-Tat-NR2B9c in the presence and absence of alteplase. Data presented as % of intact peptide; mean ± standard deviation; $n = 3$.

were acquired using a Zeiss 880 confocal microscope fitted with an cell incubation chamber. In accordance with observations that free Tat in the cytosol readily enters the nucleus and strongly binds to nucleoli,[14] homogenous staining of cytoplasm and nucleoli were considered as indicative of neuronal transduction (free accumulation of peptide, not confined to endosomes) for quantification purposes.

The results show that TAMRA-Tat alone effectively transduces neurons with 48.3% of total neurons transduced at 1 µM exposure; although dose response is minimal with only 66.8% of neurons transduced at a 10-fold higher dose of 10 µM (Fig. 3A). In contrast, TAMRA-D-Tat is significantly less effective than TAMRA-Tat at 1 µM (18.6% of cells transduced; $p < 0.0001$); but shows much better dose response than TAMRA-Tat with 89.6% of neurons transduced at 10 µM, which is significantly greater than Tat ($p < 0.001$). Mean fluorescence intensity of cells treated with TAMRA-Tat show a parallel trend where dose response is minimal, while cells treated with TAMRA-D-Tat show significantly lower uptake at 1 µM ($p < 0.0001$) but comparable uptake at 10 µM (Fig. 3B). Representative images of neurons treated with Tat-TAMRA (Fig. 3C) and D-Tat-TAMRA (Fig. 3D).

Next, we investigated whether the PPIi sequence of nerinetide (NR2B9c) contributes to the uptake of the full-length peptide into neurons by comparing neuronal transduction and uptake of TAMRA-labelled Tat and D-Tat with Tat-NR2B9c and D-Tat-NR2B9c (Fig. 4). The results show that the addition of the NR2B9c sequence to Tat results in a significant increase in neuronal transduction at 1 µM (48.3% vs. 76.3%; $p < 0.0001$) and at 10 µM exposure (66.8% vs. 88.6%; $p < 0.0001$) (Fig. 4A). Interestingly, mean fluorescence signal in neurons treated with 1 µM Tat-NR2B9c is lower than in neurons treated with 1 µM Tat ($p < 0.0001$), while mean fluorescence signal is comparable at 10 µM (Fig. 4B). These results point towards a mechanism where the addition of NR2B9c reduces the formation of endosomes but increases uptake into the cytoplasm. The addition of NR2B9c to D-Tat also results in a significant increase in neuronal transduction at 1 µM (18.6% vs. 53.1%; $p < 0.0001$),
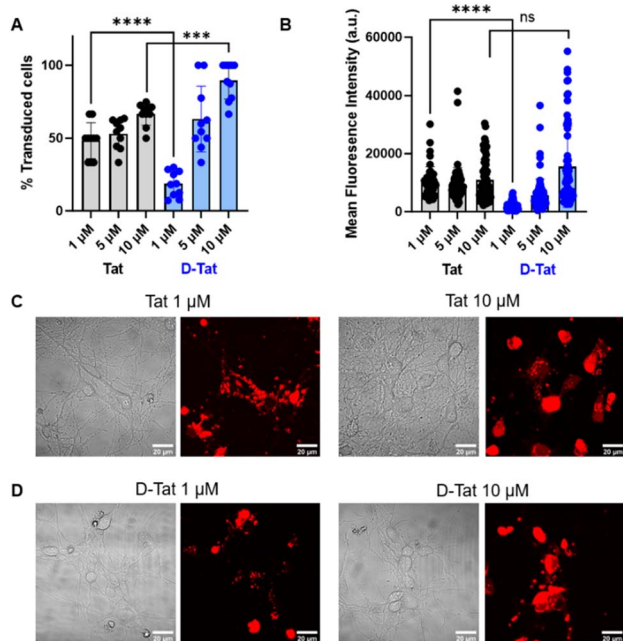


Fig. 3 Live-cell confocal microscopy of TAMRA-Tat and TAMRA-D-Tat in murine primary neurons. (A) Quantification of the percentage of transduced neurons (scored as positive when showing homogeneous cytoplasmic and nucleolar fluorescence) treated with cell penetrating peptide. (B) Quantification of average fluorescence intensity per cell in cells treated with cell penetrating peptide. (C) Brightfield and red channel images of live neurons treated with TAMRA-Tat (1 & 10 µM). (D) Brightfield and red channel images of live neurons treated with TAMRA-D-Tat (1 & 10 µM). Digital image adjustments are consistent throughout the manuscript for each concentration. Data are presented as mean ± standard deviation; n numbers are identical for each treatment group. Scale bars, 20 µm.
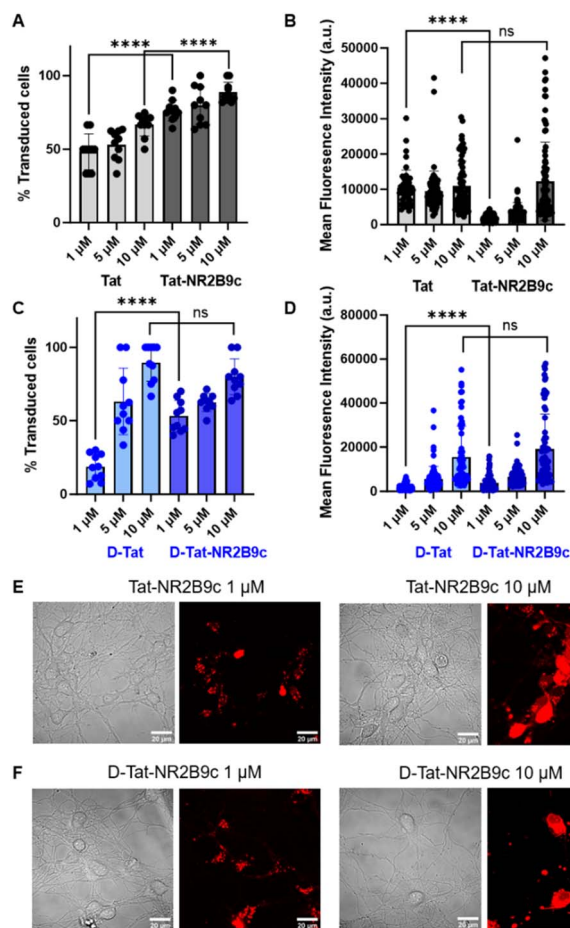


Fig. 4 Live-cell confocal microscopy of TAMRA-Tat-NRB9c and TAMRA-D-Tat-NR2B9c in murine primary neurons. (A and C) Quantification of the percentage of transduced neurons (scored as positive when showing homogeneous cytoplasmic and nucleolar fluorescence) treated with Tat vs. Tat-NR2B9c (A), D-Tat vs. D-Tat-NR2B9c (C). (B and D) Quantification of average fluorescence intensity per cell in cells treated with treated with Tat vs. Tat-NR2B9c (B), D-Tat vs. D-Tat-NR2B9c (D). (E) Brightfield and red channel images of live neurons treated with TAMRA-Tat-NR2B9c (1 & 10 µM). (F) Brightfield and red channel images of live neurons treated with TAMRA-D-Tat-NR2B9c (1 & 10 µM). Digital image adjustments are consistent throughout the manuscript for each concentration. Data are presented as mean ± standard deviation; n numbers are identical for each treatment group. Scale bars, 20 µm.

but not at 10 μM (89.6% *vs.* 79.9%; n.s.) (Fig. 4C). Mean fluorescence signal in neurons treated with 1 μM D-Tat-NR2B9c is slightly higher than in neurons treated with 1 μM D-Tat ($p <$ 0.01), with a similar trend observed at 10 μM ($p < 0.05$) (Fig. 4D). Importantly, the transduction and uptake of D-Tat-NR2B9c into neurons at 1 μM is significantly lower than that of Tat-NR2B9c (53.1% *vs.* 76.3%; $p < 0.0001$). These results confirm that D-Tat is not as effective as Tat at transducing neurons and that the PPIi section of nerinetide is not merely a cargo but enhances transport of the full-length peptide into the cytoplasm.

Finally, we investigated whether the increase in transduction and uptake observed with NR2B9c is due to the specific interaction of NR2B9c with its binding partner PSD-95. To this end we compared the uptake of TAMRA-NR2B9c with the inactive double alanine mutant TAMRA-NR2Baa (Fig. 5). Both peptides show unaided transduction of neurons (*i.e.* not requiring a dedicated CPP sequence) between 13.8% and 39.7% (1 μM and 10 μM) (Fig. 5A), but uptake into cells as indicated by mean fluorescence intensity is much lower than for any other peptide construct tested (Fig. 5B). Transduction and uptake of TAMRA-NR2B9c and TAMRA-NR2Baa is comparable at all concentrations tested, suggesting a PSD-95/NMDAR-independent mechanism. Indeed, transduction efficacy of TAMRA-Tat-NR2B9c and TAMRA-Tat-NR2Baa is comparable at all concentrations (Fig. 5C), while uptake by mean fluorescence intensity is significantly higher for TAMRA-Tat-NR2Baa at all concentration tested ($p < 0.0001$).

## Excitotoxicity assay

To investigate how stability and neuronal transduction of nerinetide work together to determine therapeutic efficacy, we utilized a neuronal protection assay.[8] In this assay, murine primary neurons are challenged with excessive NMDA (100 μM), which induces an excitotoxic signalling cascade involving the PSD-95-NMDAR PPI. Consequently, this excitotoxic treatment induces neuronal death, which is measured by propidium iodide (PI) uptake (Fig. 6A). Neurons are pre-treated with nerinetide or analogues (100 nM) to disrupt excitotoxic signal mediated by NMDAR-PSD-95 complex formation. To avoid phototoxic effects and spectral overlap with PI, we synthesized
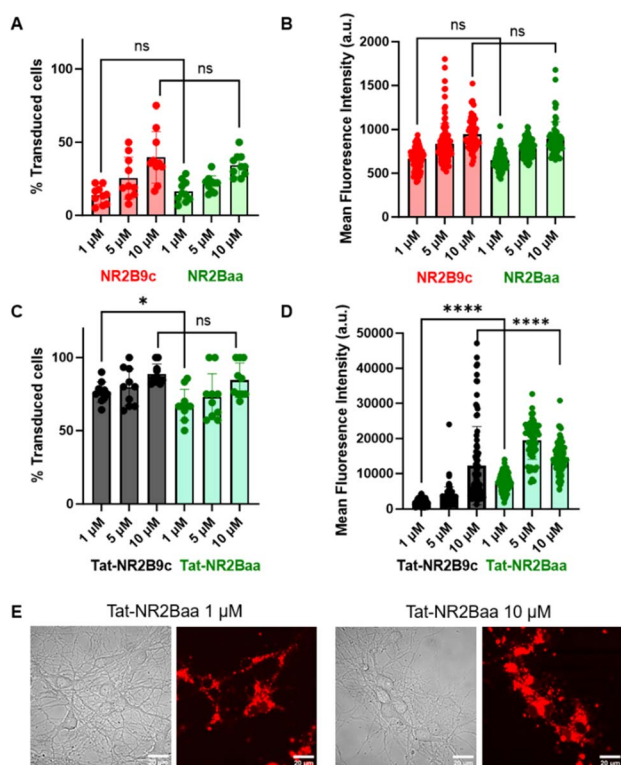


Fig. 5 Live-cell confocal microscopy of TAMRA-NRB9c, TAMRA-NR2Baa, Tat-NR2Baa in murine primary neurons. (A and C) Quantification of the percentage of transduced neurons (scored as positive when showing homogeneous cytoplasmic and nucleolar fluorescence) treated with NR2B9c *vs.* NR2Baa (A), Tat-NR2B9c *vs.* Tat-NR2Baa (C). (B and D) Quantification of average fluorescence intensity per cell in cells treated with NR2B9c *vs.* NR2Baa (B), Tat-NR2B9c *vs.* Tat-NR2Baa (D). (E) Brightfield and red channel images of live neurons treated with Tat-NR2Baa (1 & 10 μM). Digital image adjustments are consistent throughout the manuscript for each concentration. Data are presented as mean ± standard deviation; *n* numbers are identical for each treatment group. Scale bars, 20 μm.
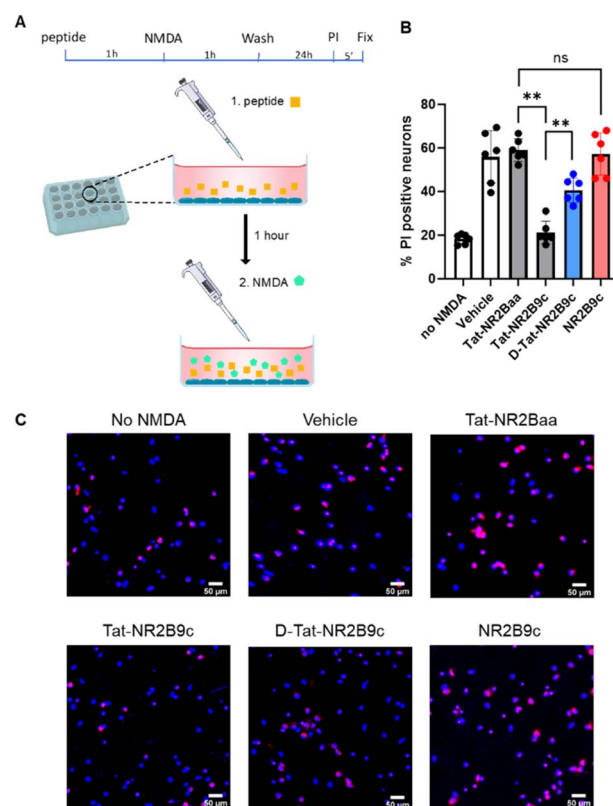


Fig. 6 Neuroprotective effect of nerinetide and analogues in excitotoxicity assay of murine primary neurons challenged with NMDA. (A and B) Excitotoxicity assay timeline and workflow – neurons are pre-treated with peptide, challenged with NMDA, number of dead neurons determined using propidium iodide. (B) Quantification of the percentage of propidium iodide-positive neurons in each treatment group. (C) Representative microscopy images of DAPI (blue)/propidium iodide (PI, purple) stained cells for each treatment group. Data are presented as mean ± standard deviation; *n* numbers are identical for each treatment group. Scale bars, 50 μm.

unlabelled peptides Tat-NR2B9c (nerinetide), D-Tat-NR2B9c, Tat-NR2Baa, and NR2B9c for this assay; none of the peptides were toxic to neurons in the absence of NMDA challenge (Fig. S1†).

Tat-NR2B9c (nerinetide) shows excellent neuroprotective properties against NMDA resulting in cell survival comparable to neurons that were not challenged with NMDA (18.9% vs. 18.3% cell death) demonstrating the excellent efficacy of nerinetide (Fig. 6B and C). The efficacy of D-Tat-NR2B9c is significantly poorer than that of Tat-NR2B9c (40.5% vs. 18.9% cell death, $p = 0.0022$), suggesting that the decrease in neuronal uptake of the D-Tat therapeutic negatively impacts its efficacy. It is important to note that lack of delivery efficacy by D-Tat is most pronounced at low concentrations ($\leq 1$ μM). As shown in the Fig. 3 and 4, neuronal uptake of peptides functionalized with D-Tat is similar or greater than those functionalized with Tat at concentrations >5 μM.

NR2B9c without a cell penetrating peptide sequence showed no neuroprotective effect, indicating that the small amount of intraneuronal delivery observed with these agents is insufficient to elicit a therapeutic response. Neurons treated with double alanine mutant known not to bind to PSD-95 – Tat-NR2Baa – showed no neuroprotective effect and resulted in cell death similar to neurons treated with NMDA only (56.9% vs. 55.9%), indicating that the neuroprotective effect of Tat-NR2B9c is mediated by the NR2B9c sequence specifically, while the Tat sequence is not directly involved in binding to PSD-95. The replacement of Tat with D-Tat in nerinetide leads to a decrease in neuroprotection by ∼60% demonstrating that lower intraneuronal delivery directly affects drug efficacy.

## Discussion

The combination of a cell penetrating peptide and a short protein mimetic peptide sequence is a powerful approach for the design of peptidic PPI inhibitors for treating CNS conditions. These agents overcome the dual challenge of delivery into the neuron and the design of effective protein–protein interaction inhibitors. By deconstructing the neuroprotective therapeutic nerinetide we elucidate the relationship between plasma stability, intraneuronal delivery and drug efficacy in this class of drug.

Clinical trials of nerinetide highlighted plasma stability problems that negatively affect drug efficacy;[10,11] the substitution of L-amino acids with D-amino acids in the cell penetrating Tat sequence significantly improves plasma stability. However, the NR2B9c sequence includes a lysine on the N-terminal (K12), adjacent to the Tat sequence, which is essential for binding to PSD-95 and cannot be substituted for a D-amino acid without loss of PSD-95 affinity.[10] Slow degradation of D-Tat-NR2B9c is likely to be attributable to protease targeting of this L-lysine residue. Further efforts to improve plasma stability, such as peptide cyclization, could be used to further improve in vivo half-life.

A surprising finding of this study is the high uptake of the Tat into neurons; Tat typically does not enter the cytosol or nucleus of commonly used cancer cells lines (HeLa, HEK, etc.) at concentrations under 10 μM.[14-16] Our results indicate that Tat is freely available in the cytosol of approximately half of treated neurons at a concentration of 1 μM, suggesting that Tat is a particularly effective cell penetrating peptide for the design of intraneuronal therapeutics. The observation that this efficacy drops significantly when D-Tat is used instead of Tat suggest that high neuronal delivery might be due to specific Tat – protein interaction, either on the cell surface or in the endosome that facilitates effective intraneuronal delivery. While the net positive charge of Tat and D-Tat is the same, D-Tat is unable to recognize specific protein motifs comprised of L-amino acids. These results suggest that the transduction efficacy of Tat in neurons is only partially attributable to the net-positive charge of the peptide.

The low concentration of peptide required for successful delivery into neurons in addition to the lack of visible membrane interaction of the TAMRA-labelled peptides tested in this study point toward an uptake mechanism that utilizes the endosomal pathway rather than direct translocation across the plasma membrane. Furthermore, addition of NR2B9c to Tat results in an improvement in transduction efficacy concurrent with an overall decrease in the amount of peptide in the neuron, which points towards an uptake mechanism where the addition of a PPIi sequence to the CPP decreases the amount to endosomally confined peptide and increases delivery into the cytoplasm. Together these observations point towards an intracellular delivery mechanism mediated by endosomal escape. We found no evidence of a PSD-95 mediated or other specific mechanism that contributes to uptake of nerinetide mediated by the NR2B9c sequence, as the delivery of PSD-95 binding NR2B9c and non-interactor NR2Baa is identical. However, the improvement in uptake when comparing Tat to Tat-NR2B9c as well as D-Tat compared to D-Tat-NR2B9c suggest that the chemical nature of the cargo sequence affects transduction and can indeed improve the intraneuronal delivery of the therapeutic agent. Both the NR2B9c and the NR2Baa sequences are charge neutral at physiological pH and have comparable lipophilicity. Our data suggest that the addition of a charge neutral cargo peptide of <10 amino acids in size improves intraneuronal delivery in comparison to the efficacy of the cell penetrating peptide by itself. While it is not possible to infer the broad applicability of this design criteria for the therapeutic sequence, our findings establish design criteria for novel first generation agents. Further improvements to the endosomal escape properties of the CPP or the use of dedicated endosomal escape peptides might further enhance the efficacy of intraneuronal deliver.

Our findings demonstrate that while plasma stability issues of Tat-containing agents can be mitigated by L to D amino acid substitution, D-Tat is significantly less effective at intraneuronal delivery at low extracellular concentrations ($\leq 1$ μM), resulting in a 60% decrease in neuroprotection with D-Tat-NR2B9c treatment at 100 nM. The resulting trade-off between stability and efficacy should be evaluated in the context of the molecular target and the clinical indication. The ESCAPE-NA1 trial showed that post-stratification of patients into alteplase treatment and non-alteplase treatment groups resulted in statistically significant therapeutic benefit of nerinetide treatment in patients that are not treated with alteplase.[9] This suggests that the improved

half-life of nerinetide in the absence of alteplase is sufficient to result in therapeutic benefit for acute stroke patients. Nonetheless, the design of novel CNS protein–protein inhibitory peptides should consider the use of cell penetrating peptides or peptide backbone structures that strike a better balance between stability and delivery efficacy. The Tat CPP sequence appears to be particularly well suited for delivery of peptides into the CNS and into neurons and could be incorporated into cyclic or natural product inspired cyclotide conformations to enhance stability without compromising on delivery efficacy.[17,18]

## Conclusions

By deconstructing the neuroprotective peptidic drug nerinetide, we derive design criteria for the improvement of nerinetide efficacy and the design of novel CNS drugs that target protein–protein interactions. Cell penetrating peptide Tat is highly effective at transporting neutrally charged cargo peptides of less than 10 amino acid in length into the cytoplasm of neurons. L to D-amino acid substitution in the Tat sequence results in improved stability but poor intraneuronal delivery and therapeutic efficacy. Future drug development efforts should focus on the use of strategies such as cyclization to improve the stability of peptide therapeutics, while maintaining efficacy.

## Data availability

The data supporting this article have been included as part of the ESI.†

## Author contributions

Conceptualization, O. T., L. I., J. v. E.; methodology, D. A., K. P., J. v. d. H., S. G., H. S., T. F.; data analysis, D. A., A. E.-O., K. P., O. T.; writing O. T., D. A.; supervision, O. T.; funding acquisition, O. T., T. F., L. I., J. v. E. All authors have read and agreed to the published version of the manuscript.

## Conflicts of interest

There are no conflicts to declare.

## Acknowledgements

## Notes and references

1 M. Muttenthaler, G. F. King, D. J. Adams and P. F. Alewood, *Nat. Rev. Drug Discovery*, 2021, **20**, 309.
2 P. McGonigle, *Biochem. Pharmacol.*, 2012, **83**, 559.
3 G. C. Terstappen, A. H. Meyer, R. D. Bell and W. Zhang, *Nat. Rev. Drug Discovery*, 2021, **20**, 362.
4 R. Blades, L. M. Ittner and O. Tietz, *J. Labelled Compd. Radiopharm.*, 2023, **66**, 237.
5 M. Aarts, Y. Liu, L. Liu, S. Besshoh, M. Arundine, J. W. Gurd, Y. T. Wang, M. W. Salter and M. Tymianski, *Science*, 2002, **298**, 846.
6 D. J. Cook, L. Teves and M. Tymianski, *Nature*, 2012, **483**, 213.
7 D. J. Cook, L. Teves and M. Tymianski, *Sci. Transl. Med.*, 2012, **4**, 154.
8 L. M. Ittner, Y. D. Ke, F. Delerue, M. Bi, A. Gladbach, J. van Eersel, H. Wölfing, *et al.*, *Cell*, 2010, **142**, 387.
9 H. C. Kornau, L. T. Schenker, M. B. Kennedy and P. H. Seeburg, *Science*, 1995, **269**, 1737.
10 M. D. Hill, M. Goyal, B. K. Menon, R. G. Nogueira, R. A. McTaggart, A. M. Demchuk, A. Y. Poppe, *et al.*, *Lancet*, 2020, **395**, 878.
11 D. Mayor-Nunez, Z. Ji, X. Sun, L. Teves, J. D. Garman and M. Tymianski, *Sci. Transl. Med.*, 2021, **13**, 1498.
12 Clinical trials: NCT04462536 (ESCAPE-NEXT); NCT02315443 (FRONTIER).
13 X. F. Zhou, *Neurosci. Bull.*, 2021, **37**, 579.
14 O. Tietz, F. Cortezon-Tamarit, R. Chalk, S. Able and K. A. Vallis, *Nat. Chem.*, 2022, **14**, 284.
15 M. P. Stewart, A. Sharei, X. Ding, G. Sahay, R. Langer and K. F. Jensen, *Nature*, 2016, **538**, 183.
16 N. Nischan, H. D. Herce, F. Natale, N. Bohlke, N. Budisa, M. C. Cardoso and C. P. Hackenberger, *Angew. Chem. Int. Ed.*, 2015, **54**, 1950.
17 P. G. Dougherty, A. Sahni and D. Pei, *Chem. Rev.*, 2019, **119**, 10241.
18 S. J. De Veer, M. W. Kan and D. J. Craik, *Chem. Rev.*, 2019, **119**, 12375.